SDC

VASCULAR COMPLEXITY ANALYSIS IN OPTICAL COHERENCE TOMOGRAPHY ANGIOGRAPHY OF DIABETIC RETINOPATHY

MINHAJ ALAM, MS,* DAVID LE, BS,* JENNIFER I. LIM, MD,† XINCHENG YAO, PHD*†

Purpose: This study aimed to verify the feasibility of using vascular complexity features for objective differentiation of controls and nonproliferative diabetic retinopathy (NPDR) and proliferative diabetic retinopathy (PDR) patients.

Methods: This was a cross-sectional study conducted in a tertiary, subspecialty, academic practice. The cohort included 20 control subjects, 60 NPDR patients, and 56 PDR patients. Three vascular complexity features, including the vessel complexity index, fractal dimension, and blood vessel tortuosity, were derived from each optical coherence tomography angiography image. A shifting-window measurement was further implemented to identify local feature distortions due to localized neovascularization and mesh structures in PDR.

Results: With mean value analysis of the whole-image, only the vessel complexity index and blood vessel tortuosity were able to classify NPDR versus PDR patients. Comparative shifting-window measurement revealed increased sensitivity of complexity feature analysis, particularly for NPDR versus PDR classification. A multivariate regression model indicated that the combination of all three vascular complexity features with shifting-window measurement provided the best classification accuracy for controls versus NPDR versus PDR.

Conclusion: Vessel complexity index and blood vessel tortuosity were the most sensitive in differentiating NPDR and PDR patients. A shifting-window measurement increased the sensitivity significantly for objective optical coherence tomography angiography classification of diabetic retinopathy.

RETINA 00:1–8, 2020

Diabetic retinopathy (DR) is a major systemic complication of diabetes and it causes hemorrhages, retinal nonperfusion, and different microvascular abnormalities in the retina.[1] With its progression from nonproliferative diabetic retinopathy (NPDR) to proliferative diabetic retinopathy (PDR), ischemia, unstable neovascularization, and complex vascular mesh can manifest, resulting in substantial damage to the retina and irreversible vision loss. Objective identification of the transition from NPDR to PDR is still challenging, especially because of the lack of quantitative features sensitive enough to track the localized morphological changes during the transition. In current clinical settings, careful monitoring of progression and reliable treatment assessments are essential steps to prevent such PDR associated vision losses.

Optical coherence tomography angiography (OCTA) facilitates quantification of capillary-level distortions due to retinopathies by providing high-resolution and depth-resolved visualization of individual retinal plexuses.[2] It has been extensively used for quantitative assessment of different retinovascular and degenerative retinal conditions.[2–8] Quantitative OCTA analysis has

From the Departments of *Bioengineering; and †Ophthalmology and Visual Sciences, University of Illinois at Chicago, Chicago, Illinois.

Supported in part by NIH grants R01EY030842, R01 EY030101, R01 EY029673, R01 EY023522, and P30 EY001792; by an unrestricted grant from Research to Prevent Blindness; by the Richard and Loan Hill endowment; by the Marion H. Schenk Chair endowment; by the Illinois Society for the Prevention of Blindness (ISPB) grant; T32AG057468 Training program in the biology and translational research on Alzheimer's disease and related dementias.

None of the authors has any conflicting interests to disclose.

Supplemental digital content is available for this article. Direct URL citations appear in the printed text and are provided in the HTML and PDF versions of this article on the journal's Web site (www.retinajournal.com).

Reprint requests: Xincheng Yao, PhD, Department of Bioengineering (MC 563), Department of Ophthalmology & Visual Sciences University of Illinois at Chicago (UIC) Clinical Sciences North, Suite W103, Room 164D 820 South Wood Street, Chicago, IL 60612; e-mail: xcy@uic.edu

also been explored for objective detection, staging, and treatment assessment of DR[9–15] and diabetic macular edema (DME).[16,17] In proliferative diabetic retinopathy (PDR), ischemic regions and vessel dropouts increase, whereas localized neovascularization and complex capillary meshes manifest in parafoveal and perifoveal regions of the retina. These visual biomarkers are commonly used by physicians qualitatively; however, quantitative OCTA analysis for objective differentiation of NPDR and PDR is yet to be validated. Some established OCTA features, such as blood vessel density (BVD), foveal avascular zone-area (FAZ-A), and foveal avascular zone-circularity index have been recently explored in quantitative analysis of PDR,[10] but these changes were not statistically significant for robust NPDR versus PDR classification. One reason for the nonsignificant result is the random localized manifestation of the complex capillary structures, which makes it very difficult to use a global OCTA feature to properly quantify retinal complexity, especially in PDR.

We hypothesized that the localized neovascularization and complex capillary meshes in the retina can be quantified as biomarkers for the detection of the transition from NPDR to PDR, which can in turn increase the overall accuracy of DR classification. Recently, the vessel complexity index (VCI) has been used as one complexity measure to quantify nonperfusion in OCTA.[18] Compared with retinal vascular structures, the background tissues have lower VCI metrics, therefore the VCI was sensitive for identifying vascular structures in the retina. However, VCI has not be used yet as a metric for measuring localized capillaries in late stage NPDR or PDR. Fractal dimension (FD)[19–23] and blood vessel tortuosity (BVT)[9,23,24] have also been used for overall structural and geometric complexity measurement of retinal vasculatures. In this study, we aimed to test these OCTA features to identify localized complexity distortions due to DR progression in the retina, and to increase OCTA feature sensitivity by using a shifting-window measurement in local retinal regions. Moreover, we used a multivariate regression model that used the vascular complexity features for OCTA differentiation of NPDR and PDR. An ensemble of vascular complexity features was able to identify NPDR progression into PDR with improved sensitivity and reliability.

Methods

Study Population and Optical Coherence Tomography Angiography Imaging

This study was a cross-sectional study of consecutive type II diabetes patients at the University of Illinois at Chicago (UIC) retina clinic. The study was approved by the institutional review board (IRB) of UIC and followed all the ethical standards stated in the Declaration of Helsinki. All 20 control subjects and 116 DR subjects (60 NPDR and 56 PDR patients) were recruited from the UIC Retinal Clinic. All patients underwent complete anterior and dilated posterior segment examination by an experienced ophthalmologist (J.I.L.). They also underwent contact lens examination with a slit-lamp to identify PDR signs. The patients were classified based on the severity of DR (mild, moderate, and severe NPDR, and PDR) according to the Early Treatment Diabetic Retinopathy Study (ETDRS) staging system. According to the American Academy of Ophthalmology, the ETDRS levels are classified as the following: no apparent retinopathy (Level 10), mild NPDR (Level 20), moderate NPDR (Level 35), severe NPDR (Level 53), and PDR (Level 61).[25] Control data were obtained from healthy volunteers without diabetes who provided informed consent for optical coherence tomography and OCTA imaging. Any eye with other retinal or ocular diseases or pathological abnormalities in the retina, such as macular edema and epiretinal membranes, were not included in this study. Additional exclusion criteria included eyes with significant macular hemorrhages, intravitreal injections, photocoagulation, and previous history of vitreoretinal surgery. To maintain homogeneity of the OCTA image database in this study, all included subjects were treatment-naïve and OCTA images were taken before treatment or intervention. About 12% of the data were excluded from the total screened and annotated NPDR and PDR data.

Spectral domain-optical coherence tomography and concurrent OCTA image data were acquired using an Angiovue SD-OCT device (Optovue, Fremont, CA) with a split-spectrum amplitude-decorrelation angiography reconstruction algorithm. Optical coherence tomography angiography scans used in this study typically had a 6-mm × 6-mm field of view that covered the perifoveal region of the retina. However, for measurement of the FAZ-A, we used 3-mm × 3-mm scans that provided a more detailed description of the fovea and its contour. Optical coherence tomography volume data were segmented to acquire OCTA images from both superficial and deep capillary plexuses (SCP and DCP) using the built-in ReVue software. In the case of moderate segmentation error, the segmentation was corrected manually. Images with severe motion and shadow artifacts were excluded.

Image Analysis

We measured three complexity quantitative features; that is, BVT, VCI, and FD. These features were

correlated and compared with BVD and FAZ-A measurements. Because PDR has localized neovascularization and mesh structures in the retina (representative images in Figure 1, A–C), we further introduced a shifting-window measurement for the vascular complexity features to increase the sensitivity of identifying PDR. For simplicity, the shifting-window dimension was chosen as 10% of the whole image dimension (300 × 300 pixels); that is, 30 × 30 pixels. A sample shifting-window is shown in Figure 1D. The window was shifted both horizontally and vertically with a 50% overlap. After shifting through the whole image, feature measurements were taken for all windows and from the shifting-window measurements. A distribution plot was created and the windows with the top 10% measurements of OCTA features were chosen. After calculating the average of these windows, averages of the maximum vascular complexity features in different groups were essentially obtained.

Before measuring the OCTA features, a binary vessel map (Figure 1E), skeleton map (Figure 1F), and perimeter map (Figure 1G) were extracted from the input images. A Hessian-based multi-scale Frangi filter[26] was used to enhance the vascular flow information.

Blood Vessel Tortuosity. The BVT was measured using segmented branches within the skeleton map (Figure 1C) in the SCP. The average BVT was measured as the ratio of the geodesic distance (curved line) to Euclidian distance (straight line) of each vessel branch.[24]

Vessel Complexity Index. Within a given window (whole image or shifting window), the VCI was calculated from the vessel perimeter map and binary vessel map[18]:

$$\mathrm{VCI} = \frac{(\text{Pixels encolsed by perimeter map})^2}{4\pi \times (\text{Pixels encolsed by vessel map})} \quad (1)$$

The VCI is a unique parameter that is able to locate the complex vascular morphology within the retina.

Fractal Dimension. Fractal dimension can quantify the degree of complexity of an object (i.e., blood vessels). In our study, the box counting technique was used to measure the FD values in both SCP and DCP. The FD analysis procedure has been described in a previous study.[24] A representative FD contour map is shown in Figure 1E.

Blood Vessel Density. Blood vessel density was measured as the percentage of the total vascular area in the retina. The binary vessel map (Figure 1B) was used to calculate the percentage of blood vessel pixels within a defined region in both SCP and DCP.

Foveal Avascular Zone-Area. The fovea was segmented and demarcated automatically (blue area in Figure 1C) using an active contour method.[24]

Statistics. Details about statistical methods used are provided in the **Supplemental Digital Content 1** (see **Supplemental Material**, http://links.lww.com/IAE/B250).

Results

The image database used in this study included 40 control eyes, 120 NPDR eyes (20 mild, 20 moderate, and 20 severe; both OD and OS from all patients) and 100 PDR eyes (both OD and OS from 44 subjects and only OD from 12 subjects), staged according to the ETDRS staging system,[25] as described in the Methods section. No statistically significant differences were present among the controls and the NPDR and PDR groups with respect to age, sex, or duration of diabetes and hypertension (analysis of variance [ANOVA], $P = 0.27$; chi-square test, $P = 0.32$). Furthermore, no significance in hypertension or insulin dependency among the stages of the NPDR and PDR groups was observed. A summary of the subject demographics and detailed univariate analysis of the quantitative OCTA features used in this study is presented in Table 1.

Univariate Analysis

A post-hoc study after the ANOVA showed that all the features were able to distinguish controls versus NPDR patients and controls versus PDR patients (Student's *t*-test, $P < 0.001$), but only VCI and BVT were able to distinguish between NPDR and PDR (Student's *t*-test, $P < 0.05$). It has been seen that FD is highly correlated with BVD when measured over the whole field of view of the OCTA image. Because of increased ischemia in severe NPDR and PDR patients, the average BVD decreased (Table 2), which in turn caused the FD values to go down. With ischemia, FAZ-A values also decreased; however, from Table 2, it can be observed that both BVD and FAZ-A were not differentiated in NPDR versus PDR.

To enhance the sensitivity of the vascular complexity features, we also conducted overlapping shifting-window measurements that provided local complexity information within the parafoveal retina. Table 1 shows that the sensitivity of the VCI, FD (SCP and DCP), and BVT increased significantly, especially when differentiating NPDR versus PDR. In this case, all vascular complexity features increased with the progression of DR (including FD), which correlated well with the vascular complexity increase in PDR. All vascular complexity features allowed differentiation of NPDR and PDR with statistical significance ($P < 0.05$). This indicated that the changes

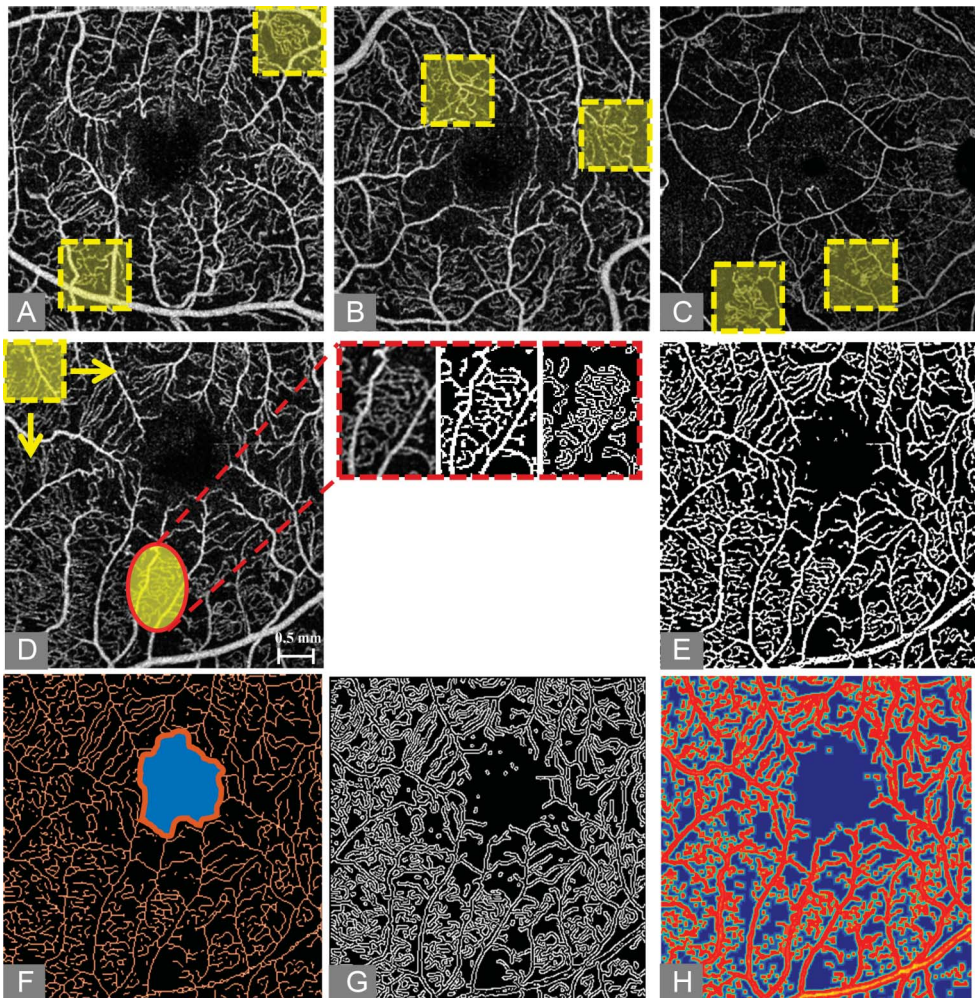

Fig. 1. Representative images. **A–C.** Examples of localized vascular complexity in PDR patients identified with shifting windows. **D–H.** Illustration of OCTA feature measurement. **A.** Optical coherence tomography angiography image from a male, 67-year-old PDR patient. The yellow circle marks a local region with vascular complexity. The region in the enlarged inset shows a corresponding vessel and perimeter map. These maps are used for measuring the local VCI values. **B.** Segmented blood vessel map. **C.** Blood vessel skeleton map with segmented fovea (marked blue region) and FAZ contour (orange boundary marked around the fovea). **D.** Vessel perimeter map. **E.** Fractal dimension contour map. Scale bar shown in A applies to all the images.

in these features were more prominent in smaller capillary regions. Compared with the vascular complexity feature analysis, BVD analysis did not increase the sensitivity of shifting-window measurements.

In addition, local complexity maps were generated for each OCTA image; sample maps from controls and NPDR and PDR OCTA images are shown in Figure 2. From the PDR map, localized complexity increments can be clearly observed.

A correlation analysis was performed to observe the relationship between the complex OCTA features and previously described OCTA features (whole image measurement); that is, BVD and FAZ-A, that differentiated NPDR and PDR[14] (Table 3). Fractal dimension

Table 1. Demographics Characteristics of Control, NPDR, and PDR Subjects

		NPDR			
	Control	Mild NPDR	Moderate NPDR	Severe NPDR	PDR
No. of subjects	20	20	20	20	56
Sex (male)	12	10	12	12	29
Age (mean ± SD)	42 ± 9.8	52.31 ± 10.22	48.05 ± 11.90	57.84 ± 11.74	56.36 ± 13.58
Age range	25–71	28–75	31–69	41–73	38–75
Duration of disease	—	14.23 ± 10.37	16.54 ± 10.08	22.32 ± 11.95	23.51 ± 10.78
Diabetes type	—	Type II	Type II	Type II	Type II
Insulin dependent (Y/N)	—	7/13	12/8	15/5	48/8
HbA1C, %	—	6.5 ± 0.6	7.3 ± 0.9	7.8 ± 1.3	8.3 ± 3.2
HTN prevalence, %	10	45	80	80	84

HbA1C, glycated hemoglobin; HTN, hypertension.

Table 2. Univariate Analysis of OCTA Features in Different Cohorts

	Whole Image Measurements						
				P			
Features	Control (I)	NPDR (II)	PDR (III)	I vs. II	II vs. III	III vs. I	ANOVA
BVT	1.10 ± 0.12	1.18 ± 0.10	1.21 ± 0.13	<0.01	0.04	<0.01	<0.01
VCI	24.15 ± 2.36	26.98 ± 3.04	30.22 ± 2.08	<0.01	0.02	<0.01	<0.01
FD_{SCP}	1.67 ± 0.29	1.62 ± 0.81	1.55 ± 0.54	<0.01	0.15	<0.01	0.029
FD_{DCP}	1.69 ± 0.35	1.63 ± 0.81	1.58 ± 0.54	<0.01	0.36	<0.01	0.032
BVD_{SCP}	49.57 ± 3.45	40.33 ± 7.28	37.85 ± 6.21	<0.01	0.24	<0.01	0.038
BVD_{DCP}	51.18 ± 4.06	40.96 ± 6.71	38.19 ± 7.34	<0.01	0.29	<0.01	0.035
FAZ_{SCP}	0.28 ± 0.17	0.38 ± 0.28	0.42 ± 0.22	<0.01	0.09	<0.01	0.022
FAZ_{DCP}	0.45 ± 0.19	0.55 ± 0.31	0.58 ± 0.26	<0.01	0.09	<0.01	0.029
	Shifting-Window Measurements						
				P			
Features	Control (I)	NPDR (II)	PDR (III)	I vs. II	II vs. III	III vs. I	ANOVA
BVT	1.15 ± 0.20	1.29 ± 0.52	1.42 ± 0.33	<0.001	<0.001	<0.001	<0.001
VCI	25.48 ± 2.24	34.73 ± 4.13	40.02 ± 4.98	<0.001	<0.001	<0.001	<0.001
FD_{SCP}	1.69 ± 0.31	1.73 ± 0.75	1.80 ± 0.82	<0.01	0.031	<0.01	<0.01
FD_{DCP}	1.68 ± 0.28	1.75 ± 0.63	1.83 ± 0.59	<0.01	0.033	<0.01	<0.01
BVD_{SCP}	55.43 ± 2.06	54.96 ± 4.15	54.01 ± 3.70	0.58	0.84	0.86	0.385
BVD_{DCP}	62.39 ± 4.65	62.84 ± 5.92	61.09 ± 5.34	0.62	0.81	0.34	0.745
FAZ_{SCP}	N/A	N/A	N/A	N/A	N/A	N/A	N/A
FAZ_{DCP}	N/A	N/A	N/A	N/A	N/A	N/A	N/A

All values are presented as mean ± SD. One-versus-one comparisons conducted using Student's *t* test. ANOVA was conducted to compare intergroup significance.

(SCP and DCP) had a statistically significant positive correlation with BVD and a negative correlation with FAZ-A, while BVT had negative correlation with BVD and positive correlation with FAZ-A. Vessel complexity index showed a negative trend with BVD and positive trend with FAZ-A but the correlation was not statistically significant. Within the vascular complexity features, only BVT and FD (SCP) showed a negative correlation ($r_s = -0.493$, $P < 0.05$).

Multivariate Analysis

A multivariate logistic regression analysis was conducted with all complexity OCTA features (both whole image and shifting-window measurements) as input features. The regression model with a backward elimination technique was initiated with all features and it eliminated them one by one depending on the prediction accuracy of the fitted regression model. The final model showed that the combination of all shifting-window measurements provided the best classification performance for control versus NPDR versus PDR classification. It could also classify the individual stages of NPDR: mild, moderate, and severe. This result further provided evidence for the importance of localized measurement of vascular complexity features. For controls versus DR, NPDR versus PDR, and control versus NPDR (including

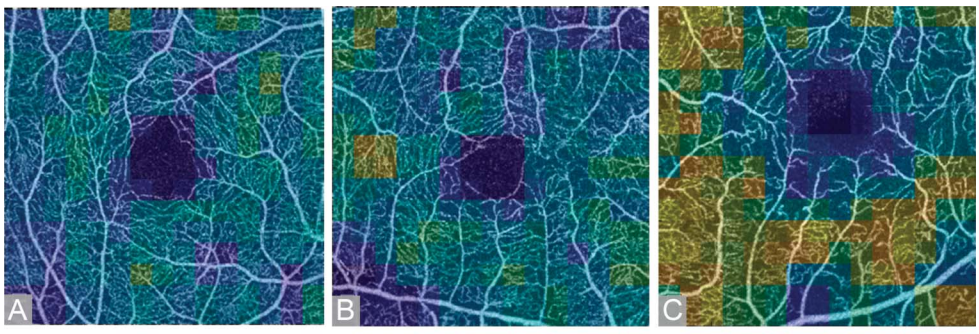

Fig. 2. Complexity map of parafoveal vasculature for (**A**) control, (**B**) NPDR, and (**C**) PDR subjects. Compared with controls and NPDR patients, the PDR OCTA image shows a localized increase in the vascular complexity of the retina.

Table 3. Correlation Analysis of Vascular Complexity Features With BVD and FAZ-A (Whole-Image Measurement)

	BVD		FAZ-A	
	r_s	P	r_s	P
BVT	−0.420	0.036	0.417	0.043
VCI	−0.186	0.089	0.214	0.064
FD_{SCP}	0.637	<0.01	−0.586	<0.01
FD_{DCP}	0.664	<0.01	−0.591	<0.01

three stages) versus PDR classification, receiver operation characteristics curves were generated (Figure 3, A–C) and the corresponding area under the receiver operation characteristics curve was also calculated. The final fitted regression model with combined features was able to classify controls versus NPDR versus PDR with 0.94 area under the receiver operation characteristics curve (94.75% sensitivity and 89.27% specificity; Figure 3D).

From Figure 3D, the regression model fitted with the combination of the complexity (shifting-window) features provided better performance metrics compared with the model fitted with individual features.

Discussion

In this study, three vascular complexity features were developed for objective OCTA classification of controls and DR cohorts. Vessel dropout and severe ischemia have been commonly observed in DR patients as the disease progresses, especially in severe NPDR and PDR stages. In PDR, ischemic regions continue to increase, causing the overall vessel density to decrease. However, there is manifestation of regional neovascularization and complex inter-twined vascular mesh structures that contribute to the overall vessel density in the perifoveal retina. Therefore, it is extremely difficult to identify the transition from severe NPDR to PDR from image-based screening alone, which further limits automated staging and classification of DR (control vs. all NPDR stages vs. PDR). Clinical treatment for PDR is more aggressive compared with NPDR treatments. Therefore, reliable identification of a PDR stage is essential for proper medical intervention. Because the capillary mesh structures and local complexity are well established clinical biomarkers of PDR, we explored vascular complexity features; that is, BVT, VCI and FD, for OCTA classification of controls and NPDR and PDR patients. Because the complexity of retinal capillaries is randomly distributed within the perifoveal retina, a shifting-window measurement was implemented to capture the localized change of the complexity features. The windows with higher metrics corresponded to regions with higher vascular complexity.

Apart from increased sensitivity for all vascular complexity features, a difference in FD analysis with shifting-window and whole-image analyses (Table 2) was observed. In general, avascular regions are assigned with small FD values whereas blood vessels are labeled with relatively high FD values. Therefore, FD has been widely used for BVD analysis.[18,23,24,27] With DR progression, the high rate of vascular dropouts results in lower vessel density; that is, a lower average number of FD values. Therefore, when FD was measured within the whole image, the value decreased from NPDR to PDR stages. Although PDR OCTA images had complex regions (local high FD values), the low vessel density values correlated to overall lower FD values within the whole OCTA image. The increased complexity was balanced out by the increased ischemic areas. However, with shifting-windows analysis, FD was able to identify regions with high complexity in PDR. Therefore, the average of the maximum FD windows increased from NPDR to PDR stages ($P < 0.05$ for NPDR vs. PDR classification), where ischemia in PDR did not affect FD measurements.

A multivariate logistic regression analysis indicated that the combination of all three vascular complexity features with shifting-window measurement showed the best classification accuracy compared with models trained with individual features (Figure 3D). The three vascular complexity features also had low correlations among each other, suggesting that these features reflect different pathological aspects of the retinal condition. The vascular complexity features were further correlated and compared with existing BVD and FAZ-A features that were previously used for DR classification.[9,10] Although BVD and FAZ-A were useful for control versus DR classification, they were not as successful for NPDR versus PDR classification. These features are able to display distortions, such as ischemia and foveal irregularities; however, these changes are often too subtle when DR progresses into PDR. The manifestation of neovascularization and complex meshes in the PDR retina cannot be defined using only BVD and FAZ-A. However, complexity metrics have been developed and designed to focus on the quantification of those complex vascular meshes, resulting in successful PDR detection. Overall control versus NPDR versus PDR classification and furthermore NPDR versus PDR staging significantly improved in our study using vascular complexity features (Table 2 and Figure 3D), compared with BVD and FAZ-A.

This study was based on a relatively small sample size available in a single imaging center. For future

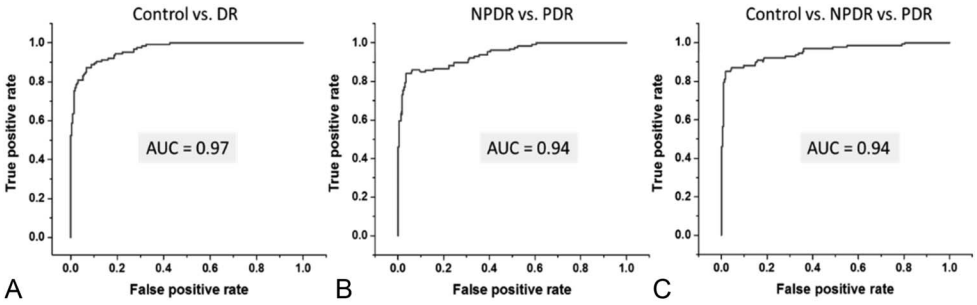

D

	Sensitivity (%)	Specificity (%)	AUC
VCI (shifting-window)	91.26	85.60	0.88
FD (shifting-window)	85.10	81.63	0.81
BVT (shifting-window)	87.62	81.34	0.86
Combined features	94.75	89.27	0.94

Fig. 3. Performance analysis of the multivariate logistic regression model for DR classification. **A–C.** Receiver operation characteristics curves illustrating classification performances of the prediction. **A.** Control versus DR. **B.** NPDR versus PDR. **C.** Control versus NPDR versus PDR (including mild, moderate, and severe NPDR stages). **D.** Comparing performances of the combined features with individual features.

study, it is desirable to involve multiple imaging centers to develop a larger OCTA database for NPDR versus PDR quantification. In addition, projection and motion artifacts in OCTA can also affect quantitative feature analysis. For this study, we excluded OCTA images with severe shadow and motion artifacts. We also excluded some images with DME that had difficulty for accurate retinal layer segmentation. Because some NPDR and PDR patients may be affected with DME simultaneously, it would be beneficial in future studies to include more DME subjects in complexity analysis. It is worth mentioning that we primarily conducted complexity analysis in the superficial layer. Even in DME affected retinas, it has been observed that superficial OCTA images retain moderate quality when analyzing local complexity features. Therefore, the clinical applicability of the complexity features should still be viable in DME affected retinas. Only 6-mm × 6-mm field of view OCTAs were available for this study to measure retinal complexity. It has been observed in previous work that neovascularization is often prevalent in the peripapillary region.[28] Radial peripapillary density has also been demonstrated as a biomarker for DR progression.[29] Therefore, it could be interesting in future studies to correlate and compare the complexity features in the peripapillary regions with other morphological changes and established biomarkers. This could also be extended to comparative analysis in multiple regions of the diseased retina. Furthermore, in our study, the NPDR-PDR staging was done using the ETDRS clinical standard. Lack of wide-field FA imaging in this study may limit the accuracy of clinical diagnosis. A comparative study of OCTA and wide-field FA imaging can be interesting to verify the accuracy of clinical diagnosis.

The adoption of complexity feature analysis in clinical practice would be beneficial for DR screening and classification, especially for identifying progression to PDR. Symptoms of PDR identified by these features could generate a referral to specialty ophthalmologists and initiate prompt intervention to prevent vision impairment. In current clinical settings, the clinical standard for DR examination is dilated indirect examination and slit-lamp biomicroscopy with noncontact lens to identify signs of PDR. Although some clinicians conduct FA to confirm PDR, it is not still a widely used practice in all clinics. Incorporating highly sensitive OCTA features, including localized complexity features, could make the screening process more efficient by providing a reference at the point-of-care environment.

Key words: vascular complexity, diabetic retinopathy, medical imaging, ophthalmology, optical coherence tomography, optical diagnostics for medicine, physiology, visual system, noninvasive assessment.

Acknowledgments

The authors thank Mr. Mark Janowicz and Ms. Andrea Degillio (Eye and Ear Infirmary, University of Illinois at Chicago) for technical support during data acquisition.

References

1. Nayak J, Bhat PS, Acharya UR, et al. Automated identification of diabetic retinopathy stages using digital fundus images. J Med Syst 2008;32:107–115.
2. Minvielle W, Caillaux V, Cohen SY, et al. Macular microangiopathy in sickle cell disease using optical coherence tomography angiography. Am J Ophthalmol 2016;164:137–144.
3. Zahid S, Dolz-Marco R, Freund KB, et al. Fractal dimensional analysis of optical coherence tomography angiography in eyes with diabetic retinopathy. Invest Ophth Vis Sci 2016;57:4940–4947.
4. Lim JI. Ophthalmic manifestations of sickle cell disease: update of the latest findings. Curr Opin Ophthalmol 2012;23: 533–536.
5. Hoang QV, Chau FY, Shahidi M, et al. Central macular splaying and outer retinal thinning in asymptomatic sickle cell patients by spectral-domain optical coherence tomography. Am J Ophthalmol 2011;151:990–994.e991.
6. Asdourian GK, Nagpal KC, Busse B, et al. Macular and perimacular vascular remodelling sickling haemoglobinopathies. Br J Ophthalmol 1976;60:431–453.
7. Condon PI, Serjeant GR. Ocular findings in homozygous sickle-cell anemia in Jamaica. Am J Ophthalmol 1972;73: 533–543.
8. Ishibazawa A, Nagaoka T, Takahashi A, et al. Optical coherence tomography angiography in diabetic retinopathy: a prospective pilot study. Am J Ophthalmol 2015;160:35–44.
9. Alam M, Zhang Y, Lim JI, et al. Quantitative optical coherence tomography angiography features for objective classification and staging of diabetic retinopathy. Retina 2020;40:322–332.
10. Ashraf M, Nesper PL, Jampol LM, et al. Statistical model of optical coherence tomography angiography parameters that correlate with severity of diabetic retinopathy. Invest Ophth Vis Sci 2018;59:4292–4298.
11. Cao D, Yang D, Huang Z, et al. Optical coherence tomography angiography discerns preclinical diabetic retinopathy in eyes of patients with type 2 diabetes without clinical diabetic retinopathy. Acta Diabetol 2018;55:469–477.
12. Dimitrova G, Chihara E, Takahashi H, et al. Quantitative retinal optical coherence tomography angiography in patients with diabetes without diabetic retinopathy. Invest Ophth Vis Sci 2017;58:190–196.
13. Hwang TS, Jia Y, Gao SS, et al. Optical coherence tomography angiography features of diabetic retinopathy. Retina (Philadelphia, PA) 2015;35:2371.
14. Li Z, Alzogool M, Xiao J, et al. Optical coherence tomography angiography findings of neurovascular changes in type 2 diabetes mellitus patients without clinical diabetic retinopathy. Acta Diabetol 2018;55:1075–1082.
15. Lin TC, Gogte P, Palejwala N, et al. Quantitative spectral-domain optical coherence tomography angiography (OCTA) of diabetic retinopathy (DR) severity. Invest Ophth Vis Sci 2017;58:1653.
16. Falavarjani KG, Iafe NA, Hubschman JP, et al. Optical coherence tomography angiography analysis of the foveal avascular zone and macular vessel density after anti-VEGF therapy in eyes with diabetic macular edema and retinal vein occlusion. Invest Ophth Vis Sci 2017;58:30–34.
17. Hsieh YT, Alam MN, Le D, et al. Optical coherence tomography angiography biomarkers for predicting visual outcomes after ranibizumab treatment for diabetic macular edema. Ophthalmol Retina 2019;3:826–834.
18. Chu Z, Lin J, Gao C, et al. Quantitative assessment of the retinal microvasculature using optical coherence tomography angiography. J Biomed Opt 2016;21:066008.
19. Agarwal A, Aggarwal K, Akella M, et al. Fractal dimension and optical coherence tomography angiography features of the central macula after repair of rhegmatogenous retinal detachments. Retina 2019;39:2167–2177.
20. Corvi F, Pellegrini M, Erba S, et al. Reproducibility of vessel density, fractal dimension, and foveal avascular zone using 7 different optical coherence tomography angiography devices. Am J Ophthalmol 2018;186:25–31.
21. Dave VP, Pappuru RR, Gindra R, et al. OCT angiography fractal analysis-based quantification of macular vascular density in BRVO eyes. Can J Ophthalmol 2019;54:297–300.
22. Gadde SG, Anegondi N, Bhanushali D, et al. Quantification of vessel density in retinal optical coherence tomography angiography images using local fractal dimension. Invest Ophth Vis Sci 2016;57:246–252.
23. Alam M, Thapa D, Lim JI, et al. Computer-aided classification of sickle cell retinopathy using quantitative features in optical coherence tomography angiography. Biomed Opt express 2017;8:4206–4216.
24. Alam M, Thapa D, Lim JI, et al. Quantitative characteristics of sickle cell retinopathy in optical coherence tomography angiography. Biomed Opt Express 2017;8:1741–1753.
25. International Council of Ophthalmology. International clinical diabetic retinopathy disease severity scale. Available at: http://www.icoph.org/dynamic/attachments/resources/diabetic-retinopathy-detail.pdf. Accessed June 5, 2019.
26. Frangi AF, Niessen WJ, Vincken KL, et al. Multiscale vessel enhancement filtering. Paper presented at: International Conference on Medical Image Computing and Computer-Assisted Intervention. Berlin, Germany: Springer, 1998. pp. 130–137.
27. Alam MN, Zhang Y, Lim JI, et al. Quantitative OCT angiography for computer-aided classification of diabetic retinopathy. Invest Ophth Vis Sci 2018;59.